

Special Session 3: Seismic Data Acquisition and Processing in Mountainous Thrust Areas

Thursday morning, October 27th

3-D acquisition realities and processing strategies in mountainous thrust areas

Scott MacKay*, Stuart Wright, James Gaiser, Alex Jackson, Craig Beasley, and Daniel Wisecup, *Western Geophysical*

SS3.1

Summary

The inherent structural complexity of thrust plays makes them ideal candidates for 3-D seismic imaging. However, there are many practical constraints placed on the acquisition of 3-D data in the mountainous terrains typically associated with thrust regimes. Financial considerations can result in tradeoffs between a desired acquisition geometry and that which is practical. Topographic relief can also impose irregular geometries and shortened receiver arrays. Such factors create challenges to the formation of a valid 3-D seismic image. Therefore, the realities of acquiring data in mountainous areas must be coupled to the appropriate processing strategies to yield an optimal result.

Short Arrays and Prestack Noise Suppression

Rugged topography is typical of thrust environments. Therefore, to reduce the filtering action of the receiver array on primary data, it is common practice to use short, contoured arrays. Unfortunately, short arrays also minimize the attenuation of shot-generated coherent noise. To solve such noise problems on 2-D data we commonly use methods such as $f-k$ filtering. However, the irregular sampling in azimuth and offset, found in most land 3-D surveys, often precludes the use of 2-D methodologies. Additionally, directional variations in array response and azimuthal variations in the noise itself imply that data-adaptive methods are preferable for robust noise attenuation.

One solution to the coherent noise suppression problem is an $f-x$ domain technique that derives a least-squares estimate of the coherent noise from the data within a user-defined range of dips. The modeled noise may then be subtracted from the shot record. In practice, shot records are binned into azimuth ranges and then grouped by increasing offset. Each azimuthally-ordered record is individually analyzed for coherent noise. Figure 1a is a shot record showing the 11 azimuth bins (12.5 degree increment) with the greatest cross-line orientation. The sudden jumps in the mute pattern correspond to gaps in the offset sampling. Here, a range of dips was defined that spanned the steeply-dipping noise visible on the records. Figure 1b shows the least-squares estimate of the coherent noise within the specified dip range. The amount of coherent noise present in the data appears greater than a casual inspection of the shot records would initially indicate. Finally, Figure 1c is the shot record with the coherent noise subtracted.

Acquisition Geometry and Refraction/Reflection Statics

The problem of reflection-static decoupling may be present to some extent in all 3-D surveys. Static decoupling, commonly seen as a trace-to-trace jitter in the CMP stack, is usually symptomatic of unresolved long-wavelength statics. More precisely, the lack of statistical overlap from one CMP trace to the next in the long-wavelength static solution gives the appearance of a high-frequency static problem, especially when the stacked data are viewed as 2-D profiles. In reality, adjacent CMP traces have converged on different and incorrect structural solutions. 3-D decoupling problems, as manifested by this CMP jitter, may be effectively addressed by the application of a running-average or so-called coupling filter on the structural term during the residual-statics

solution. Although the obvious jitter disappears, the resultant smooth structural shape still contains unresolved long-wavelength static errors. Since the 3-D structural term may be coupled during processing, yet still contain long-wavelength errors, it is clearly inappropriate to design a survey with the sole idea of solving the decoupling problem.

Figure 2a shows a common 3-D geometry with a 50 ms static anomaly located approximately at the center of the survey. The anomaly was introduced to a noise-free synthetic dataset derived from the acquisition geometry. The data were properly corrected for normal moveout prior to 10 iterations of 3-D Gauss-Seidell residual-statics decomposition. Ideally, an exact solution to the static anomaly would be derived, leaving no structural errors in the stacked response. However, Figure 2b shows a maximum structural error of approximately 10 ms and many sudden steps (decoupling jitter) in the structural-error surface when the coupling filters are not used. With the coupling filters applied, the structural-error surface (Figure 2c) is smooth (coupled) but still shows a maximum structural error of 5 ms.

The results above are consistent with those derived from modeling a range of geometries (Wisecup, 1994) and confirm that realistic acquisition geometries alone cannot address static decoupling caused by unresolved long-wavelength static problems. The appropriate methodology is to design surveys to support 3-D refraction static solutions in order to minimize the long-wavelength static errors.

Irregular/Coarse Geometries and DMO

Understanding the amplitude and phase characteristics of a reflector is often vital for prospect delineation. Therefore, the acquisition geometry should not affect the results of an important step in imaging such as dip moveout (DMO). DMO is a wave-equation method that eliminates CMP smear and the influence of dip on stacking velocities. The application of DMO is similar to migration in that each input sample is placed at all the locations appropriate for a full range of dips. However, poor sampling in offset or azimuth can cause an inconsistency in dip content after DMO that may result in phase and amplitude distortions. Fortunately, DMO is a well-defined process and a simple normalization scheme can effectively correct for the distortions (Beasley and Klotz, 1992). By tabulating the number of live dip components contributed from each azimuth and offset to each output sample, the appropriate equalization correction may be applied.

Figure 3a is a DMO stack of synthetic data having an irregular geometry caused by missing shots. Notice the amplitude and phase errors caused by applying conventional DMO. However, by applying equalized DMO (EQ-DMO) we obtain the improved results shown in Figure 3b. The equalization process for DMO is also a valuable aid in the design of 3-D acquisition geometries. Since the equalization tables are derived from the field geometry, attributes that indicate appropriate sampling for DMO may be evaluated prior to acquisition (Beasley, 1993).

Wide-azimuth Geometries and the Velocity/Statics Loop

It is often desirable to maximize the receiver effort when acquiring data in mountainous terrains. This typically results in a wide-azimuth geometry. However, wide-azimuth geometries impact the iterative approach to velocity analysis and reflection statics. The basic problem is that stacking velocities are affected by the apparent dip of reflectors (Levin, 1971). Since apparent dip is a function of structural dip and source-receiver azimuth, no single velocity will flatten a midpoint gather if azimuth is ignored in the normal moveout equation (Lehmann and Houba, 1985). Furthermore, reflection-static solutions will be compromised by this inability to flatten the data. Although DMO would eliminate the effect of apparent dip on velocities, it would also destroy the surface consistency of the data and our ability to perform residual reflection statics.

A method of reducing the effects of apparent dip may be illustrated using a synthetic dataset. The field geometry is a single 3-D cell consisting of four evenly spaced source-receiver azimuths with the same range of offsets. The reflectors consist of five planar events with a dip of 30 degrees. The dip direction of the reflectors varies evenly from north (at 5 seconds) to south (at 2.5 seconds) and velocities increase smoothly with depth. Figure 4a is a velocity analysis at the cell midpoint. Notice that there are three velocity maxima at each time. The distinct maxima are a result of the acquisition and reflector geometries. One azimuth is dip oriented, having the maximum dip-affected velocity. Another azimuth is strike oriented, having no dip effect and the lowest velocity. The other two azimuths yield the higher-semblance central peak. Clearly, no single velocity function can flatten the gather using the standard normal moveout equation and the subsequent application of reflection statics would be compromised.

Although the consequences of varying apparent dip are severe, the solution is simple. Since we know the geometry of the survey, i.e. the azimuths involved, knowledge of the reflector geometry would allow for a simple calculation of the traveltimes differences that give rise to the dip-affected velocities. Therefore, we derive a 3-D dipfield from the in-line and cross-line stacks using the same multichannel semblance process employed by most interpolation programs. Given the reflector geometry, it is now possible to correct the data within a gather for the dip effect on traveltimes and velocities via dynamic time shifts. By removing the dip effect in this manner, the surface-consistency of the seismic data is preserved- a critical consideration for subsequent reflection statics. Figure 4b shows the velocity analysis after correcting the data for apparent dip. A single velocity function will now flatten the gather and yield an optimal statics solution. Finally, the statics solution is applied to the original data prior to DMO. As an additional benefit, the velocities derived above represent the "flat-layer" velocities appropriate for moveout correction prior to DMO.

Topographic Relief and Datuming

Thrust regimes are typically associated with mountainous terrains. However, many steps in processing involve placing the data at a horizontal datum. These datuming steps are typically implemented by vertical time shifts. Unfortunately, one of the least appreciated aspects of seismic data processing is the deleterious effect of using such vertical time shifts to perform datum corrections. This is especially true when wave-equation based methods such as DMO and migration are involved. The reason is quite simple; seismic

waves do not propagate as vertical shifts. Therefore, distortions are introduced to the data that are inconsistent with the wave-equation methods to follow. The results can be unpredictable.

Fortunately, methods of damming seismic data that honor the wave equation are available (Berryhill, 1979, MacKay, 1994). Such methods may be efficiently implemented in the processing flow and eliminate potential distortions on the final seismic image. Figure 5a is the migrated result of data shifted from the recording surface (shown dashed) to the datum (at 0 seconds). In the case of Figure 5a, a wave-equation based damming approach was used and the results are accurate. Figure 5b shows the results of migration after a datum shift using vertical time shifts. Notice the false structural picture that results.

Conclusions

Many practical constraints are placed on the acquisition of 3-D data in mountainous terrains. However, processing techniques are available to solve many problems created by 3-D land geometries. *F-x* coherent noise suppression is effective for shot records with irregular offset sampling and azimuthally-varying noise. Amplitude and phase errors, introduced by the application of conventional DMO, may be reduced by an equalized DMO procedure. The velocity/statics loop, complicated by a varying dip effect to velocity in a wide-azimuth geometry, may be simplified by using a data-derived dipfield to correct for apparent dip. Using an appropriate datuming methodology can avoid compromising data prior to DMO or migration. Finally, although processing solutions exist that can couple the residual-statics solution, it is apparent that decoupling is merely symptomatic of the underlying long-wavelength statics problem. Therefore, a practical approach in survey design is to ensure proper sampling for 3-D refraction statics.

REFERENCES

- Beasley, C., and Klotz, R., 1992, Equalization of DMO for irregular spatial sampling: 62nd Ann. Internat. Mtg., Soc. Expl. Geophys., Expanded Abstracts, 970-973.
- Beasley, C., 1993, Quality assurance of spatial sampling for DMO: 63rd Ann. Internat. Mtg., Soc. Expl. Geophys., Expanded Abstracts, 544-547.
- Berryhill, J. R., 1979, Wave-equation datuming: *Geophysics* 44, 1329-1344.
- Lehmann, H. J., and Houba, W., 1985, Practical aspects of the determination of 3-D stacking velocities: *Geophysical Prospecting* 33, 34-51.
- Levin, F. K., 1971, Apparent velocity from dipping interface reflections: *Geophysics* 36, 510-516.
- MacKay, S., 1994, Efficient wavefield extrapolation to irregular surfaces using finite differences: Zero-velocity damming: 64th Ann. Internat. Mtg., Soc. Expl. Geophys., Expanded Abstracts, (these proceedings).
- Wisecup, R. Daniel, 1994, The relationship between 3-D acquisition geometry and 3-D static corrections: 64th AM. Internat. Mtg., Soc. Expl. Geophys., Expanded Abstracts, (these proceedings).

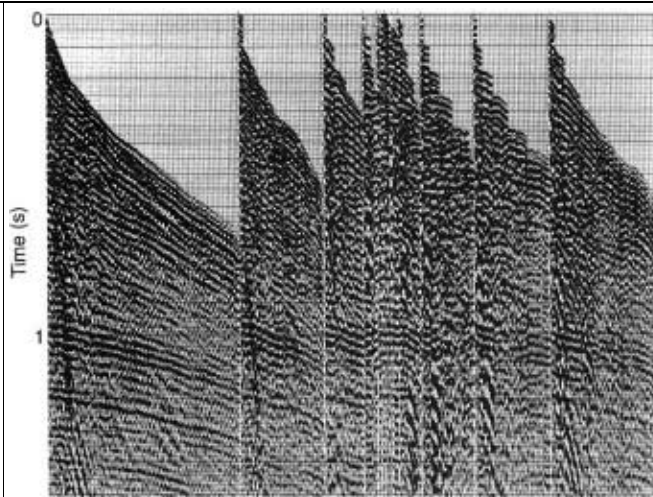


Figure 1a 3-D shot record sorted by azimuth, then offset. Eleven azimuth bins (12.5 degree increment) displayed.

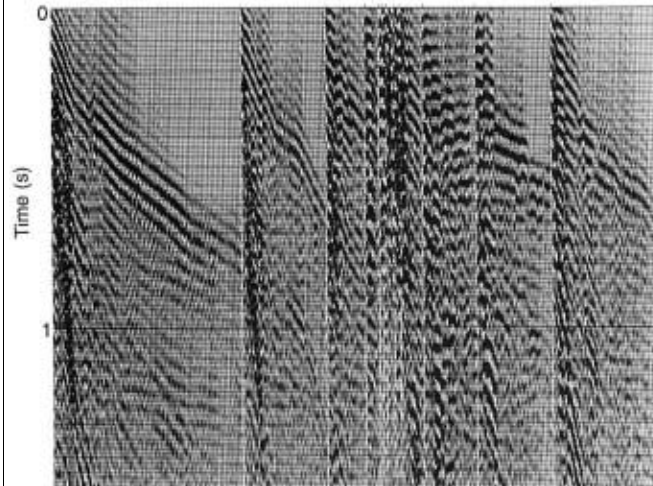


Figure 1b Coherent noise estimate of 3-D shot record in Figure 1a. Each azimuth was analyzed independently.

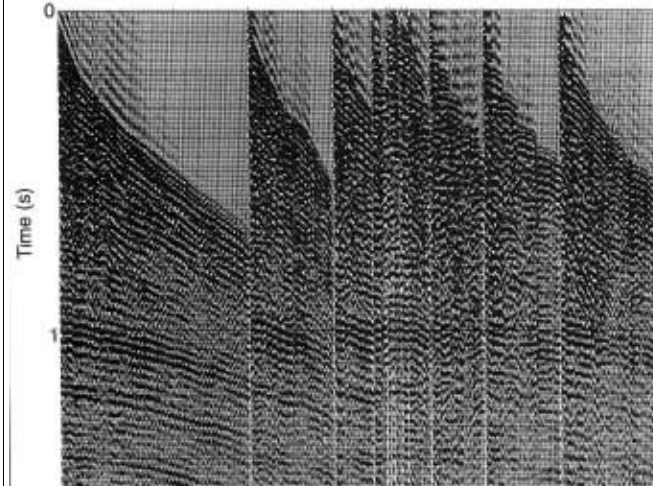


Figure 1c 3-D shot record of Figure 1a with coherent noise (Figure 1b) subtracted.

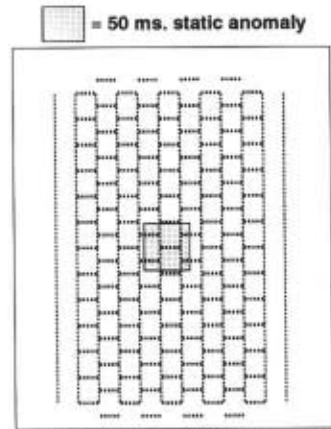


Figure 2a Common 3-D survey design showing a 50 ms static anomaly located approximately at the center of the survey.

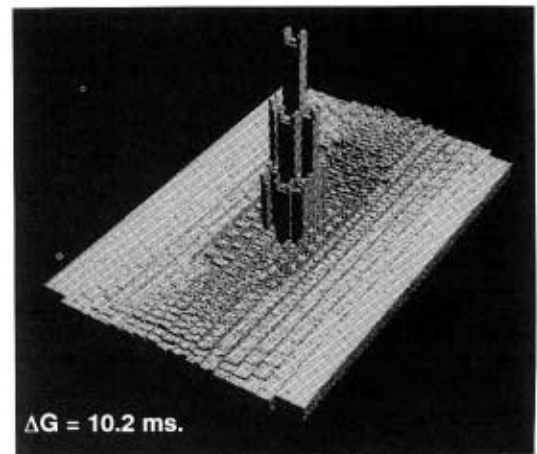


Figure 2b Structural-error surface (G) of (decoupled) residual-statics solution for geometry in Figure 2a. Note the maximum error of approximately 10 ms and the many sudden steps (decoupling jitter).

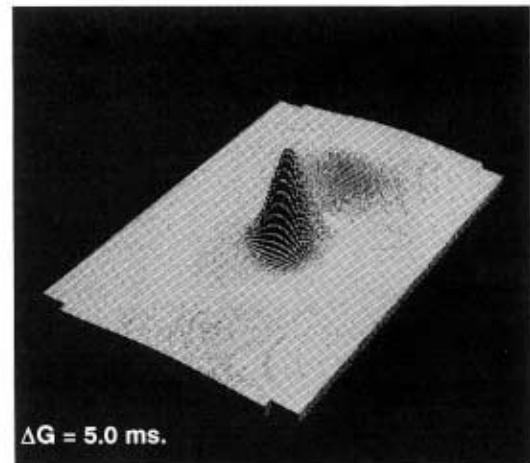


Figure 2c Structural-error surface of (coupled) residual-statics solution for geometry in Figure 2a. Note the maximum error of approximately 5 ms and the smooth nature of the error surface.

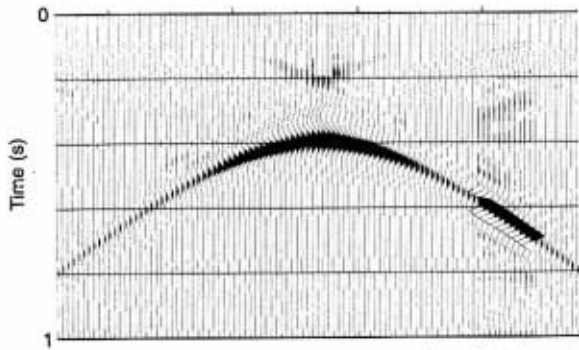


Figure 3a Stack after DMO without equalization. Missing shots have caused amplitude and phase distortions in the data.

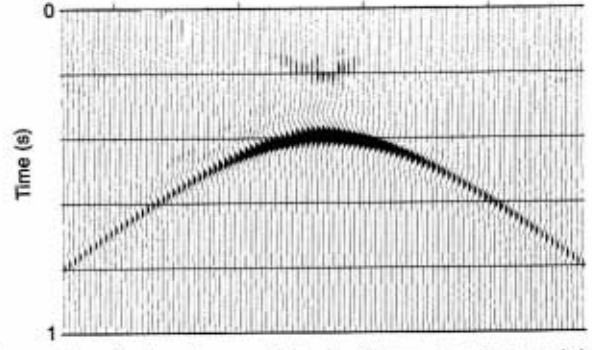


Figure 3b Stack of same data in Figure 3a after applying equalized DMO (EQ-DMO).

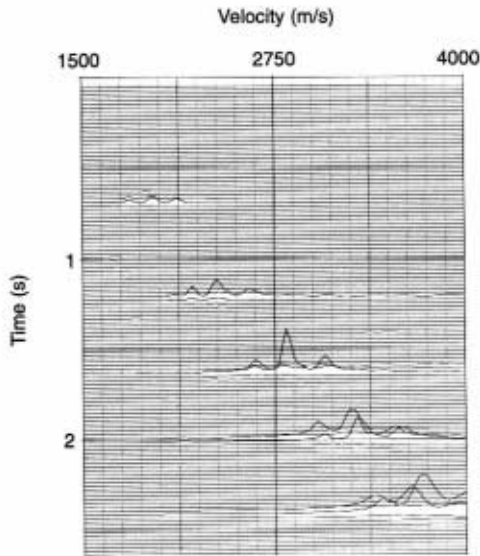


Figure 4a Velocity analysis from a wide-azimuth geometry over a series of beds dipping at 30 degrees with varying strike. Note the lack of a single semblance maximum at each time.

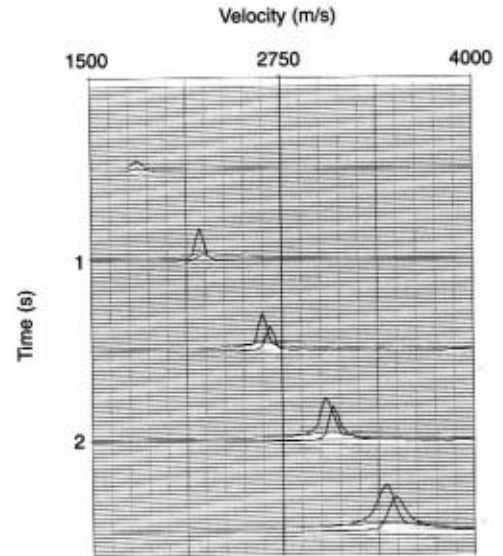


Figure 4b The same data in Figure 4a after correcting the input data for the effects of apparent dip.

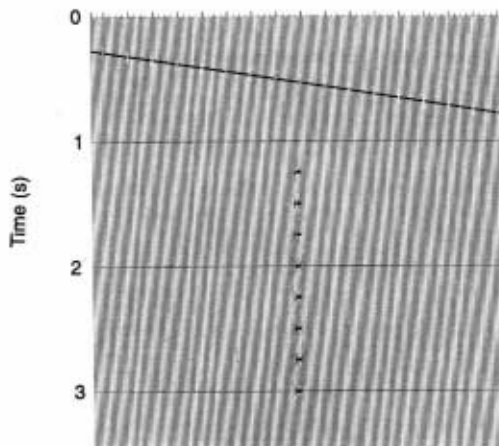


Figure 5a Accurate migration of data shifted from the recording surface (shown dashed) to the datum (0 seconds) using a wave-equation datuming approach.

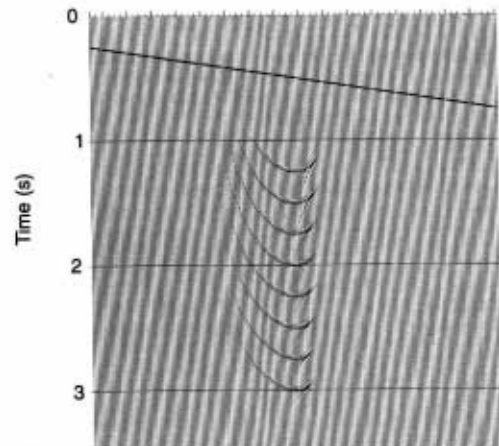


Figure 5b Distorted migration of data using vertical datum shifts.